Quantum Advantage of Ranging via Squeezed States

Bünyamin Kartal[1], Stefano Marano[2], Andrea Conti[3], and Moe Z. Win[4]

[1]*Quantum neXus Laboratory, Massachusetts Institute of Technology, USA*
[2]*Department of Information & Electrical Engineering and Applied Mathematics (DIEM), University of Salerno, Italy*
[3]*Department of Engineering and CNIT, University of Ferrara, Italy*
[4]*Laboratory for Information and Decision Systems, Massachusetts Institute of Technology, USA*

***Abstract*—Quantum ranging is crucial in several applications such as radar and localization. This paper determines the quantum advantage of ranging with single-mode displaced squeezed states. Exact analytical expressions for the quantum Fisher information (QFI) about the range parameter are derived in the presence of thermal loss channels characterized by arbitrary loss and noise parameters. The quantum advantage, termed as gain, is determined as a ratio of QFI with and without employing squeezing. It is shown that the gain can be unboundedly large in the optical regime whereas it is upper bounded in the microwave regime.**

***Index Terms*—Ranging, quantum Fisher information, squeezed states, quantum estimation.**

I. Introduction

Quantum technologies may provide substantial performance improvements in various fields such as sensing, communication, and control, compared to their classical counterparts [1]–[6]. Among the quantum technologies, quantum photonics emerged as a prominent candidate for many applications since photons weakly interact with their environment, making them more resilient to decoherence with respect to other alternatives [7]–[9]. Within quantum photonics, entangled and squeezed light sources have been key enablers to realize the quantum advantage [4], [10], [11].

Quantum photonics has found applications in radar, lidar, and quantum illumination. The advantage provided by quantum systems for ranging and Doppler parameter estimation are examined in [12] and [13] where the authors show that employing a two-mode squeezed vacuum state can lead to substantial performance gains compared to classical states. The advantage provided by employing displaced squeezed states in joint range and velocity estimation is examined in [14], which shows that Heisenberg scaling is attainable using homodyne measurement. The works [15]–[18] on quantum illumination examine under various settings the quantum advantage provided by two-mode squeezed state on target detection while the work [19] provides analytical expressions of the quantum Fisher information (QFI) for phase estimation in single-mode Gaussian metrology and derives the optimal Gaussian measurement systems.

Most of the works in the literature consider two-mode squeezed light and employ a retained idler as a key enabler for quantum advantage for quantum illumination and quantum radar. These scenarios correspond to a passive form of ranging where the reflected waveform together with the stored idler is used. In active ranging, the goal is to extract the maximum amount of information from the received waveform where both the transmitting and receiving parties cooperate. In this case, the (retained) idler cannot be used by the receiver, which makes two-mode squeezing not suitable for active ranging.

It has been shown that quantum technologies may bring substantial improvements in range and velocity estimation [12], [13], [20].[1] In the literature the quantum advantage has been investigated assuming particular forms of background radiation for given levels of loss and noise. In particular, two regimes have been mainly investigated: the optical and the microwave frequency regime. In the optical frequency regime, the effect of the background radiation can be mostly neglected, and photon loss represents the main source of performance impairment. In the microwave frequency regime, the background radiation significantly affects the system performance. Deriving the QFI in the presence of thermal loss channels characterized by any loss and noise levels is a challenging task, which makes the investigation of the quantum advantage an elusive goal in many cases of practical interest.

The fundamental questions related to active quantum ranging are: What is the quantum advantage offered by quantum states under different loss and noise conditions, and how should quantum states be designed to maximize the Fisher information about the parameter to be estimated? The answers to these questions will enable the design of active-ranging systems with quantum technologies and provide guidelines on which situations these technologies should be adopted. This paper determines the quantum advantage for active ranging of monochromatic single-mode Gaussian states. In particular, the key contributions of this paper are as in the following.

- We determine the theoretical limits of range estimation with single-mode monochromatic Gaussian states in the presence of general thermal loss channels.
- We analyze the quantum advantage provided by monochromatic displaced squeezed states in optical as well as microwave frequency regime.

Notation: Random variables are displayed in sans serif, upright fonts; their realizations in serif, italic fonts. Matrices and operators are denoted by bold uppercase letters. The

The fundamental research described in this paper was supported, in part, by the National Science Foundation under Grant CCF-1956211, the Ministero dell'Università e della Ricerca and NextGenerationEU under Grant No. 2022JES5S2, and the Robert R. Taylor Professorship. *Corresponding author: Moe Z. Win (e-mail:* `moewin@mit.edu`*).*

[1]For classical radiation sources, the fundamental limits of active ranging and localization can be found in [21]–[23].

979-8-3315-3159-1/25/$31.00 ©2025 IEEE
DOI 10.1109/QCNC64685.2025.00066

rotation matrix is defined as $\boldsymbol{R}(\theta) = \begin{bmatrix} \cos(\theta) & -\sin(\theta) \\ \sin(\theta) & \cos(\theta) \end{bmatrix}$ for $\theta \in [0, 2\pi)$. The set of non-negative integers, real numbers, and complex numbers are denoted by $\mathbb{N}_0$, $\mathbb{R}$, and $\mathbb{C}$, respectively. The imaginary unit is $\imath = \sqrt{-1}$. The symbols $\mathfrak{L}(\mathcal{H})$ and $\mathfrak{B}(\mathcal{H})$ denote the set of linear operators and bounded linear operators on a Hilbert space $\mathcal{H}$, respectively. For two operators $\boldsymbol{A}, \boldsymbol{B} \in \mathfrak{L}(\mathcal{H})$, $[\![\boldsymbol{A}, \boldsymbol{B}]\!]_- = \boldsymbol{A}\boldsymbol{B} - \boldsymbol{B}\boldsymbol{A}$ denotes their commutator. For an operator $\boldsymbol{A} \in \mathfrak{L}(\mathcal{H})$ the Hermitian is denoted by $\boldsymbol{A}^\dagger$, and for a scalar $z \in \mathbb{C}$ the complex conjugate is denoted by $z^\dagger$.

II. Preliminaries

This section first presents background material on continuous variable systems, then introduces the definitions of displaced squeezed states, and finally discusses the properties of the thermal loss channel. The underlying Hilbert space $\mathcal{H}$ is separable and infinite dimensional. For a monochromatic electromagnetic wave, the Hamiltonian describing the system is given by [8]

$$\boldsymbol{H} = \frac{\boldsymbol{P}^2 + \omega_0^2 \boldsymbol{Q}^2}{2} = \hbar\,\omega_0(\boldsymbol{A}^\dagger \boldsymbol{A} + \boldsymbol{I}/2)\,, \tag{1}$$

where ω_0 is the angular frequency of the monochromatic wave, $\hbar$ is the reduced Planck constant, $\boldsymbol{Q} \in \mathfrak{L}(\mathcal{H})$ and $\boldsymbol{P} \in \mathfrak{L}(\mathcal{H})$ are respectively the canonical position and momentum observables that satisfy the commutation relationship $[\![\boldsymbol{Q}, \boldsymbol{P}]\!]_- = \imath\hbar\,\boldsymbol{I}$, while $\boldsymbol{A} = (\omega_0 \boldsymbol{Q} + \imath \boldsymbol{P})/\sqrt{2\hbar\,\omega_0} \in \mathfrak{L}(\mathcal{H})$ and $\boldsymbol{A}^\dagger \in \mathfrak{L}(\mathcal{H})$ are respectively the field annihilation and creation operators that satisfy the commutation relationship $[\![\boldsymbol{A}, \boldsymbol{A}^\dagger]\!]_- = \boldsymbol{I}$. The observable $\boldsymbol{N} \triangleq \boldsymbol{A}^\dagger \boldsymbol{A} \in \mathfrak{L}(\mathcal{H})$ is called the number observable whose eigenkets $\{|n\rangle,\, n \in \mathbb{N}_0\}$ form a basis for $\mathcal{H}$ and satisfy

$$\boldsymbol{N}|n\rangle = n|n\rangle\,, \qquad n \in \mathbb{N}_0\,. \tag{2}$$

The eigenket $|n\rangle$ describes a quantum state with n photons, which is referred to as the number state. The action of the annihilation and creation operator on number states is respectively described by the following relations for $n \in \mathbb{N}_0$:[2]

$$\boldsymbol{A}|n\rangle = \sqrt{n}\,|n-1\rangle \quad \text{and} \quad \boldsymbol{A}^\dagger|n\rangle = \sqrt{n+1}\,|n+1\rangle\,. \tag{3}$$

A. Displaced Squeezed States

For single-mode optics, the generation and manipulation of light is mainly accomplished by the operations of displacement and squeezing.[3] Upon their application to the vacuum state, the displacement operator and squeezing operator form coherent states and squeezed states, respectively. The displacement operator $\boldsymbol{D}(\alpha_\mathrm{d}) \in \mathfrak{B}(\mathcal{H})$ is defined to be

$$\boldsymbol{D}(\alpha_\mathrm{d}) \triangleq \exp\{\alpha_\mathrm{d} \boldsymbol{A}^\dagger - \alpha_\mathrm{d}^\dagger \boldsymbol{A}\}\,, \tag{4}$$

where $\alpha_\mathrm{d} = r_\mathrm{d}\, e^{\imath\phi_\mathrm{d}} \in \mathbb{C}$, $r_\mathrm{d} \in [0, \infty)$, and $\phi_\mathrm{d} \in [-\pi, \pi)$. The displacement operator is unitary with $\boldsymbol{D}^\dagger(\alpha_\mathrm{d}) = \boldsymbol{D}(-\alpha_\mathrm{d})$. The application of the displacement operator to the vacuum state $|0\rangle$ gives coherent states

$$|\alpha_\mathrm{d}\rangle \triangleq \boldsymbol{D}(\alpha_\mathrm{d})\,|0\rangle = e^{-\frac{r_\mathrm{d}^2}{2}} \sum_{n=0}^{\infty} \frac{\alpha_\mathrm{d}^n}{\sqrt{n!}} |n\rangle\,. \tag{5}$$

Coherent states, also called quasi-classical states, are used to model classical radiation and are eigenstates of the annihilation operator $\boldsymbol{A}|\alpha_\mathrm{d}\rangle = \alpha_\mathrm{d}\,|\alpha_\mathrm{d}\rangle$. The effect of the displacement operator $\boldsymbol{D}(\alpha_\mathrm{d})$ on the annihilation operator $\boldsymbol{A}$ is described by

$$\boldsymbol{D}^\dagger(\alpha_\mathrm{d})\boldsymbol{A}\,\boldsymbol{D}(\alpha_\mathrm{d}) = \boldsymbol{A} + \alpha_\mathrm{d}\boldsymbol{I}\,, \tag{6}$$

which shows that the displacement operator displaces the annihilation operator along the direction specified by α_d.

Another form of monochromatic wave is described by squeezed states in which the variance of one of the quadratures is reduced and the variance of the conjugate quadrature is increased. The squeezing operator $\boldsymbol{S}(\alpha_\mathrm{s}) \in \mathfrak{B}(\mathcal{H})$ is defined to be the unitary operator

$$\boldsymbol{S}(\alpha_\mathrm{s}) \triangleq \exp\left\{\frac{1}{2}\left(\alpha_\mathrm{s}^\dagger \boldsymbol{A}^2 - \alpha_\mathrm{s} {\boldsymbol{A}^\dagger}^2\right)\right\} \in \mathfrak{B}(\mathcal{H})\,, \tag{7}$$

where $\alpha_\mathrm{s} = r_\mathrm{s}\, e^{\imath\phi_\mathrm{s}} \in \mathbb{C}$, $r_\mathrm{s} \in [0, \infty)$, and $\phi_\mathrm{s} \in [-\pi, \pi)$. The application of the squeezing operator $\boldsymbol{S}(\alpha_\mathrm{s})$ to the vacuum state $|0\rangle$ gives squeezed states

$$|\alpha_\mathrm{s}\rangle \triangleq \boldsymbol{S}(\alpha_\mathrm{s})\,|0\rangle\,. \tag{8}$$

The effect of the squeezing operator $\boldsymbol{S}(\alpha_\mathrm{s})$ on the annihilation operator $\boldsymbol{A}$ is described by

$$\boldsymbol{S}^\dagger(\alpha_\mathrm{s})\boldsymbol{A}\boldsymbol{S}(\alpha_\mathrm{s}) = \cosh(r_\mathrm{s})\boldsymbol{A} - e^{\imath\phi_\mathrm{s}}\sinh(r_\mathrm{s})\boldsymbol{A}^\dagger\,. \tag{9}$$

For $\phi_\mathrm{s} = 0$, the effect of squeezing on quadrature operators is described by[4]

$$\boldsymbol{S}^\dagger(\alpha_\mathrm{s})\boldsymbol{Q}\boldsymbol{S}(\alpha_\mathrm{s}) = e^{-r_\mathrm{s}}\boldsymbol{Q}\,, \tag{10a}$$

$$\boldsymbol{S}^\dagger(\alpha_\mathrm{s})\boldsymbol{P}\boldsymbol{S}(\alpha_\mathrm{s}) = e^{r_\mathrm{s}}\boldsymbol{P}\,, \tag{10b}$$

which show that one of the quadratures is reduced and the other is increased. The effects of squeezing and displacement can be combined to make a displaced squeezed state.[5]

$$|\alpha(\alpha_\mathrm{s}, \alpha_\mathrm{d})\rangle \triangleq \boldsymbol{D}(\alpha_\mathrm{d})\boldsymbol{S}(\alpha_\mathrm{s})|0\rangle\,. \tag{11}$$

The displaced squeezed states form the most general form of pure Gaussian states for a single-mode field, see Appendix A. The phase-space representation of a displaced squeezed state is illustrated in Figure 1a.

In classical mechanics, the system evolution is described in terms of canonical variables in the phase-space representation. In such a representation, each point in the phase-space refers to the exact value of a canonical variable. In quantum mechanics, canonical variables are promoted to canonical observables ($\boldsymbol{P}$ and $\boldsymbol{Q}$), and the Heisenberg uncertainty relation precludes the

[2] In (3), $\boldsymbol{A}|0\rangle$ is understood to be the null ket, i.e., the $\boldsymbol{0}$ vector of $\mathcal{H}$.

[3] The most generic state description also involves rotation operations. However, the effect of rotation operators can be absorbed into the displacement and squeezing operations [11].

[4] The quadrature operators considered in the phase-space are dimensionless quadrature operators with $\boldsymbol{Q} = (\boldsymbol{A} + \boldsymbol{A}^\dagger)/\sqrt{2}$ and $\boldsymbol{P} = (\boldsymbol{A} - \boldsymbol{A}^\dagger)/\sqrt{2}\imath$ that satisfy the commutation relationship $[\![\boldsymbol{Q}, \boldsymbol{P}]\!]_- = \imath\boldsymbol{I}$.

[5] By introducing a different parametrization, the reversed order of the two operations in (11) could also be considered. Defining $\lambda = \cosh(|\alpha_\mathrm{s}|)$ and $\nu = -\sinh(|\alpha_\mathrm{s}|)e^{\imath\phi_\mathrm{s}}$, one gets $|\alpha(\alpha_\mathrm{s}, \alpha_\mathrm{d})\rangle = \boldsymbol{S}(\alpha_\mathrm{s})\boldsymbol{D}(\alpha_\mathrm{d}\lambda - \alpha_\mathrm{d}^\dagger\nu)|0\rangle$ [11].

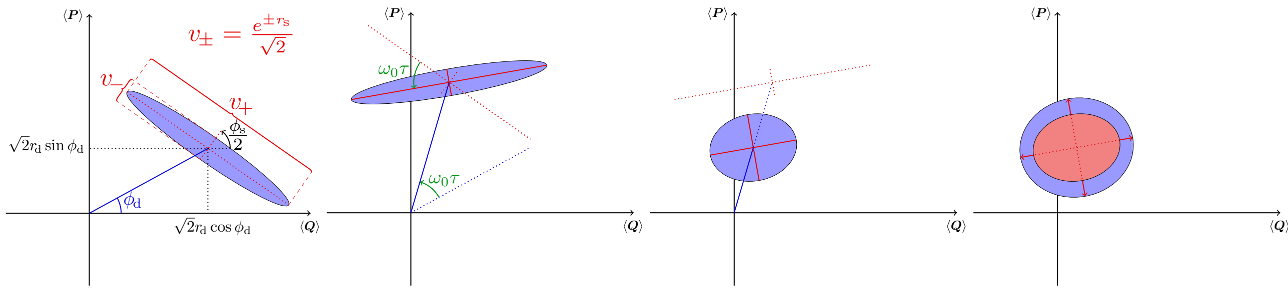

(a) (b) (c) (d)

Fig. 1: Phase-space representation of a Gaussian state. Plot (a): transmitted displaced squeezed state $|\alpha(\alpha_{\mathrm{s}}, \alpha_{\mathrm{d}})\rangle$. Plot (b): received state under the ideal channel conditions $\kappa = 1, \bar{n} = 0$; the effect of the phase rotation on mean value and squeezing angle is indicated by the green arrows. Plot (c): effect of an only-loss channel with $\kappa = 1/4, \bar{n} = 0$; this channel reduces the effect of squeezing and pulls the mean down to the origin. Plot (d): effect of a thermal loss channel with $\kappa = 1/4, \bar{n} = 1$; with respect to the case shown in (c), the standard deviations of the canonical operators increase.

exact knowledge of both canonical operators since they do not commute. Then, a point in the phase-space description is replaced by an ellipse whose center is the mean value of the canonical observables with respect to the underlying quantum state, and whose diameters in the direction of the ellipse major and minor axes denote the standard deviation of the observables in that direction. For example, the horizontal direction may refer to the standard deviation of the position observable with respect to the underlying quantum state and then the vertical direction refers to the momentum observable.

B. Thermal Loss Channel

The Bogoluibov transformation enables to describe the receiver's field annihilation operator $\boldsymbol{A}_{\mathrm{r}} \in \mathfrak{L}(\mathcal{H})$ as a function of the transmitter's field annihilation operator $\boldsymbol{A}_{\mathrm{s}} \in \mathfrak{L}(\mathcal{H})$ and the background radiation's annihilation operator $\boldsymbol{A}_{\mathrm{b}} \in \mathfrak{L}(\mathcal{H})$. The Bogoluibov transformation for thermal loss channel is[6] [3]

$$\boldsymbol{A}_{\mathrm{r}} = \sqrt{\kappa}\, e^{\imath \omega_0 \tau} \boldsymbol{A}_{\mathrm{s}} + \sqrt{1-\kappa}\, \boldsymbol{A}_{\mathrm{b}} \,, \tag{12}$$

where $1 - \kappa \in [0, 1]$ characterizes the propagation loss experienced by the signal and τ is an unknown propagation time to be estimated for ultimately inferring the range $R \triangleq c\,\tau$, with c denoting the speed of light. The relation (12) describes the action of a quantum channel whose input and output are, respectively, $\boldsymbol{A}_{\mathrm{s}}$ and $\boldsymbol{A}_{\mathrm{r}}$, while the background radiation described by $\boldsymbol{A}_{\mathrm{b}}$ represents the noise contribution. The background radiation is in a thermal state with average number of photons $\bar{n}/(1-\kappa)$, where[7]

$$\bar{n} = \frac{1}{\exp\{\hbar\, \omega_0 / (k_{\mathrm{B}} T)\} - 1} \tag{13}$$

in which k_{B} is the Boltzmann constant and T is the temperature at the receiver in Kelvins. The effect of the quantum channel described by (12) on the mean vector $\boldsymbol{d}$ and covariance matrix $\boldsymbol{V}$ of a Gaussian state is [3]

$$\boldsymbol{d} \;\longrightarrow\; \sqrt{\kappa}\, \boldsymbol{R}(\omega_0 \tau)\, \boldsymbol{d} \,, \tag{14a}$$

$$\boldsymbol{V} \;\longrightarrow\; \kappa\, \boldsymbol{R}(\omega_0 \tau) \boldsymbol{V} \boldsymbol{R}^{T}(\omega_0 \tau) + \frac{(2\,\bar{n} + 1 - \kappa)}{2} \boldsymbol{I} \,, \tag{14b}$$

where the elements of $\boldsymbol{V}$ and $\boldsymbol{d}$ are provided in Appendix A.

The effect of the phase delay, propagation loss, and thermal noise in the phase-space representation is illustrated in Figures 1b, 1c, and 1d, respectively. It can be seen that the propagation loss decreases the mean value and the amount of squeezing of the quadratures, whereas the noise increases the variance of quadratures isotropically.

III. Quantum Advantage for Ranging

For single-mode monochromatic waves, the coherent state $|\alpha_{\mathrm{d}}\rangle$ behaves as a classical electromagnetic field since the measurement of electric field observable gives the same results as in the classical theory. To produce a quantum effect, the squeezing is needed. This section determines the quantum advantage provided by the squeezing operation in estimating the unknown parameter τ, with such an advantage expressed in terms of the QFI. First, the QFI is derived for general displaced squeezed states, then the analysis focuses on the important cases of optical and microwave frequency regimes.

For a displaced squeezed state $|\alpha(\alpha_{\mathrm{s}}, \alpha_{\mathrm{d}})\rangle$, the received state is a Gaussian state with mean vector and covariance matrix given, respectively, by

$$\boldsymbol{d} = \sqrt{2\kappa} \begin{bmatrix} r_{\mathrm{d}} \cos(\omega_0 \tau + \phi_{\mathrm{d}}) \\ r_{\mathrm{d}} \sin(\omega_0 \tau + \phi_{\mathrm{d}}) \end{bmatrix} , \tag{15a}$$

$$\boldsymbol{V} = \frac{1}{2} \boldsymbol{R}\left(\omega_0 \tau + \frac{\phi_{\mathrm{s}}}{2}\right) \begin{bmatrix} v_- & 0 \\ 0 & v_+ \end{bmatrix} \boldsymbol{R}^{\mathrm{T}}\left(\omega_0 \tau + \frac{\phi_{\mathrm{s}}}{2}\right) , \tag{15b}$$

where $v_{\pm} = \kappa\,(e^{\pm 2 r_{\mathrm{s}}} - 1) + 2\,\bar{n} + 1$.

The average number of photons for a state described by the density operator $\boldsymbol{\Xi}$ is given by $\bar{n}_{\mathrm{tx}} \triangleq \mathrm{Tr}\{\boldsymbol{\Xi} \boldsymbol{A}^{\dagger} \boldsymbol{A}\}$ and represents the total excitation energy – a measure of the system resources. For the displaced squeezed state, the

[6]In (12), the channel phase information is assumed to be known and only phase introduced by the propagation is considered.

[7]The division by $1 - \kappa$ rules out possible "shadow effects" or "passive signatures" of the thermal radiation [24].

density operator is given by $\boldsymbol{\Xi} = |\alpha(\alpha_\mathrm{s}, \alpha_\mathrm{d})\rangle\langle\alpha(\alpha_\mathrm{s}, \alpha_\mathrm{d})|$ and the average number of photons $\bar{n}_\mathrm{tx}$ is given by the sum of individual contributions related to squeezing $(\sinh^2(r_\mathrm{s}))$ and displacement (r_d^2) operations:

$$\bar{n}_\mathrm{tx} = \sinh^2(r_\mathrm{s}) + r_\mathrm{d}^2\,. \tag{16}$$

Let $\gamma \triangleq \sinh^2(r_\mathrm{s})/\bar{n}_\mathrm{tx}$ and $1-\gamma = r_\mathrm{d}^2/\bar{n}_\mathrm{tx}$ be the fractions of system resources allocated to perform the squeezing and the displacement operations, respectively. The next sections address the optimal resource allocation problem that maximizes the system performance with respect to γ for a fixed $\bar{n}_\mathrm{tx}$.

A. Quantum Fisher information

Appendices B and C provide details for the calculation of QFI about the parameter τ for a displaced squeezed state described by $\boldsymbol{\Xi} = |\alpha(\alpha_\mathrm{s}, \alpha_\mathrm{d})\rangle\langle\alpha(\alpha_\mathrm{s}, \alpha_\mathrm{d})|$. In this case the QFI is given by

$$J(\tau) = \frac{32\,\kappa^2\omega_0^2\left(\sinh^4(r_\mathrm{s}) + \sinh^2(r_\mathrm{s})\right)}{1 + (2\,\bar{n}+1)^2 + 4\,\kappa\,(2\,\bar{n}+1-\kappa)\,\sinh^2 r_\mathrm{s}} + 4\,\kappa\,\omega_0^2\,r_\mathrm{d}^2\left(\frac{\sin^2(\phi_\mathrm{eq})}{v_+} + \frac{\cos^2(\phi_\mathrm{eq})}{v_-}\right), \tag{17}$$

where $\phi_\mathrm{eq} \triangleq \phi_\mathrm{d} - \phi_\mathrm{s}/2 - \pi/2 \in (-\pi, \pi]$. Since $v_+ \geqslant v_- > 0$, the QFI is maximized by setting $\phi_\mathrm{eq} = 0$ or $\phi_\mathrm{eq} = \pi$, e.g., by setting $\phi_\mathrm{d} = 0, \phi_\mathrm{s} = -\pi$. Thus, the maximum over $\phi_\mathrm{eq} \in (-\pi, \pi]$ of the QFI in (17) is given by

$$J(\tau;\gamma,\bar{n}_\mathrm{tx}) \triangleq \frac{32\,\kappa^2\omega_0^2\,\gamma\,\bar{n}_\mathrm{tx}(1+\gamma\,\bar{n}_\mathrm{tx})}{1 + (2\,\bar{n}+1)^2 + 4\,\kappa\,(2\,\bar{n}+1-\kappa)\,\gamma\,\bar{n}_\mathrm{tx}} + \frac{4\,\kappa\,\omega_0^2\,(1-\gamma)\,\bar{n}_\mathrm{tx}}{\kappa\left(e^{-2\,\mathrm{asinh}(\sqrt{\gamma\,\bar{n}_\mathrm{tx}})} - 1\right) + 2\,\bar{n} + 1}, \tag{18}$$

where the definition of γ has been employed. The "gain" is defined to be[8]

$$G(\tau;\gamma,\bar{n}_\mathrm{tx}) \triangleq \frac{J(\tau;\gamma,\bar{n}_\mathrm{tx})}{J(\tau;0,\bar{n}_\mathrm{tx})}, \tag{19}$$

where the denominator represents the QFI corresponding to the single operation of displacement, which is $J(\tau;0,\bar{n}_\mathrm{tx}) = 4\,\kappa\,\omega_0^2\,\bar{n}_\mathrm{tx}/(2\,\bar{n}+1)$.

The aim of the optimal resource allocation is to maximize the QFI over γ for a fixed value of $\bar{n}_\mathrm{tx}$. The optimal QFI and the corresponding optimal gain are respectively given by

$$J^\star(\tau;\bar{n}_\mathrm{tx}) \triangleq \max_{\gamma\in[0,1]} J(\tau;\gamma,\bar{n}_\mathrm{tx})\,, \tag{20a}$$

$$G^\star(\tau;\bar{n}_\mathrm{tx}) \triangleq \max_{\gamma\in[0,1]} G(\tau;\gamma,\bar{n}_\mathrm{tx})\,, \tag{20b}$$

and are achieved by

$$\gamma^\star \triangleq \operatorname*{argmax}_{\gamma\in[0,1]} J(\tau;\gamma,\bar{n}_\mathrm{tx})\,. \tag{21}$$

Two wavelength regimes that deserve special attention are: (i) the optical regime, in which the background radiation satisfies $\bar{n} \ll 1$; and (ii) the microwave regime, in which the background radiation satisfies $\bar{n} \gg 1$. The QFI in these two regimes is considered next.

[8]Thus, a quantum advantage is obtained if $G(\gamma,\bar{n}_\mathrm{tx}) > 1$.

B. Quantum advantage in optical regime

Employing (18) and imposing $\bar{n} \ll 1$, the QFI in the optical regime can be written as[9]

$$J_\mathrm{o}(\tau;\gamma,\bar{n}_\mathrm{tx}) = \frac{16\,\kappa^2\omega_0^2\gamma\,\bar{n}_\mathrm{tx}(\gamma\,\bar{n}_\mathrm{tx}+1)}{1 + 2\,\kappa\,(1-\kappa)\,\gamma\,\bar{n}_\mathrm{tx}} + \frac{4\,\kappa\,\omega_0^2\,(1-\gamma)\bar{n}_\mathrm{tx}}{\kappa\left(e^{-2\,\mathrm{asinh}(\sqrt{\gamma\,\bar{n}_\mathrm{tx}})} - 1\right) + 1}\,. \tag{22}$$

Note that the first term of the QFI depends only on the squeezing contribution $\gamma\,\bar{n}_\mathrm{tx}$, whereas the second term depends on both the squeezing contribution $\gamma\,\bar{n}_\mathrm{tx}$ and the displacement contribution $(1-\gamma)\bar{n}_\mathrm{tx}$. According to (19), the quantum gain results in

$$G_\mathrm{o}(\tau;\gamma,\bar{n}_\mathrm{tx}) = \frac{4\,\kappa\,\gamma\,(\gamma\,\bar{n}_\mathrm{tx}+1)}{1 + 2\,\kappa\,(1-\kappa)\,\gamma\,\bar{n}_\mathrm{tx}} + \frac{(1-\gamma)}{\kappa\left(e^{-2\,\mathrm{asinh}(\sqrt{\gamma\,\bar{n}_\mathrm{tx}})} - 1\right) + 1}\,. \tag{23}$$

In the limit for $\bar{n}_\mathrm{tx} \to \infty$ with any $\gamma \in (0,1]$ we have

$$\lim_{\bar{n}_\mathrm{tx}\to\infty} G_\mathrm{o}(\tau;\gamma,\bar{n}_\mathrm{tx}) = \frac{2\,\gamma}{1-\kappa} + \frac{1-\gamma}{1-\kappa}\,, \tag{24}$$

where the relations $\gamma\,\bar{n}_\mathrm{tx} \gg 1$ and $e^{-2\,\mathrm{asinh}(\sqrt{\gamma\,\bar{n}_\mathrm{tx}})} \ll 1$ are used. Expression (24) is maximized when $\gamma \to 1$ which shows that for large $\bar{n}_\mathrm{tx}$ the optimal strategy consists of allocating all the system resources to perform squeezing. On the other hand, the limit for $\bar{n}_\mathrm{tx} \to 0$, with $\gamma \in (0,1]$ gives

$$\lim_{\bar{n}_\mathrm{tx}\to 0} G_\mathrm{o}(\tau;\gamma,\bar{n}_\mathrm{tx}) = 4\,\kappa\,\gamma + 1 - \gamma\,, \tag{25}$$

showing that allocating all of the system resources to squeezing is advantageous when $\kappa > 1/4$.

For $\kappa = 1$, i.e., in the ideal condition with no propagation loss, (23) yields

$$G_\mathrm{o}(\tau;\gamma,\bar{n}_\mathrm{tx})\Big|_{\kappa=1} = 4\gamma\,(\gamma\,\bar{n}_\mathrm{tx}+1) + (1-\gamma)e^{2\,\mathrm{asinh}(\sqrt{\gamma\,\bar{n}_\mathrm{tx}})}\,,$$

that for $\gamma = 1$ reduces to

$$G_\mathrm{o}(\tau;1,\bar{n}_\mathrm{tx})\Big|_{\kappa=1} = 4\,(\bar{n}_\mathrm{tx}+1)\,. \tag{26}$$

C. Quantum advantage in microwave regime

Employing (18) and $\bar{n} \gg 1$, the QFI in the microwave regime can be written as

$$J_\mu(\tau;\gamma,\bar{n}_\mathrm{tx}) = \underbrace{\frac{8\,\kappa^2\omega_0^2\,\gamma\,\bar{n}_\mathrm{tx}(1+\gamma\,\bar{n}_\mathrm{tx})}{\bar{n}\left(\bar{n} + 2\,\kappa\,\gamma\,\bar{n}_\mathrm{tx}\right)}}_{\text{squeezing}} + \underbrace{\frac{2\,\kappa\,\omega_0^2\,(1-\gamma)\,\bar{n}_\mathrm{tx}}{\bar{n}}}_{\text{displacement}}. \tag{27}$$

In (27), the two contributions of the displacement and squeezing operations are separated. Maximizing (27) over γ yields

$$J_\mu^\star(\tau;\bar{n}_\mathrm{tx}) = \begin{cases} \frac{8\,\kappa^2\omega_0^2\,\bar{n}_\mathrm{tx}(\bar{n}_\mathrm{tx}+1)}{\bar{n}\,(\bar{n}+2\,\kappa\,\bar{n}_\mathrm{tx})} & \text{if } 2\,\kappa\,\bar{n}_\mathrm{tx} > \bar{n} \\ \frac{2\,\kappa\,\omega_0^2\,\bar{n}_\mathrm{tx}}{\bar{n}} & \text{if } 2\,\kappa\,\bar{n}_\mathrm{tx} \leqslant \bar{n}\,. \end{cases} \tag{28}$$

[9]In the following, the subscript "o" will be appended to quantities that refer to the optical regime while the subscript "μ" will be appended to quantities that refer to the microwave regime.

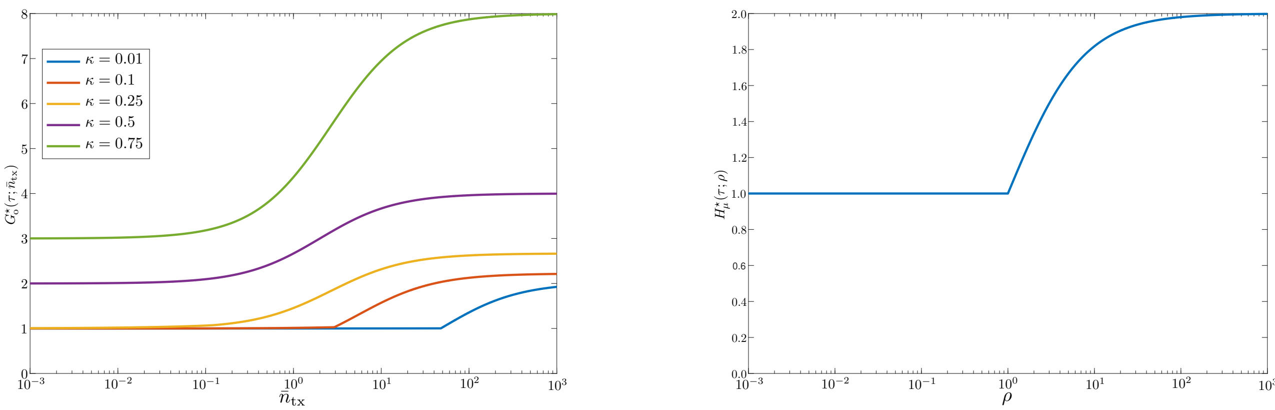

(a)

(b)

Fig. 2: Quantum advantage. Plot (a): $G_{\mathrm{o}}^{\star}(\tau;\bar{n}_{\mathrm{tx}})$ versus $\bar{n}_{\mathrm{tx}}$ in the optical regime with frequency 400 THz. Plot (b) $H_{\mu}^{\star}(\tau;\rho)$ versus ρ in the microwave regime with frequency 300 MHz.

Expression (28) reveals that the Fisher information is maximized by allocating all the system resources to perform either the squeezing operation only (if $2\,\kappa\,\bar{n}_{\mathrm{tx}} > \bar{n}$) or the displacement operation only (otherwise).

Since $\bar{n} \gg 1$, in the case that $2\,\kappa\,\bar{n}_{\mathrm{tx}} > \bar{n}$, one has $\bar{n}_{\mathrm{tx}}+1 \approx \bar{n}_{\mathrm{tx}}$. Using such an approximation and introducing the signal-to-noise ratio (SNR)

$$\rho \triangleq \frac{2\,\kappa\,\bar{n}_{\mathrm{tx}}}{\bar{n}}\,, \tag{29}$$

the optimal QFI in (28) can be expressed as a function of ρ:

$$I_{\mu}^{\star}(\tau;\rho) = \begin{cases} \omega_0^2\,\frac{2\rho^2}{\rho+1} & \text{if } \rho > 1\,, \\ \omega_0^2\,\rho & \text{if } \rho \leqslant 1\,, \end{cases} \tag{30}$$

where $I_{\mu}^{\star}(\tau;\rho) = J_{\mu}^{\star}(\tau;\rho\,\bar{n}/(2\kappa))$. Expression (30) shows that the optimal QFI is proportional to ω_0^2, proportional to the SNR for $\rho \leqslant 1$, and approximately proportional to the SNR for $\rho \gg 1$. In particular, the optimal QFI obtained for $\rho \gg 1$ is twice the optimal QFI obtained for $\rho < 1$.

Posing $H_{\mu}^{\star}(\tau;\rho) = G_{\mu}^{\star}(\tau;\rho\,\bar{n}/(2\kappa))$ for the optimal gain as function of the SNR ρ, yields

$$H_{\mu}^{\star}(\tau;\rho) = \begin{cases} \frac{2\rho}{\rho+1} & \text{if } \rho > 1 \\ 1 & \text{if } \rho \leqslant 1\,. \end{cases} \tag{31}$$

Since $1 \leqslant H_{\mu}^{\star}(\tau;\rho) < 2$, the gain is upper bounded by two.

D. Numerical Results

A quantum advantage is achieved when the QFI obtained by employing displaced squeezed states is larger than the QFI obtained by employing displaced-only states that do not encompass any genuinely quantum effect. Depending on the operating conditions, such a quantum advantage can be substantial.

Figure 2a shows the optimal gain in the optical regime $G_{\mathrm{o}}^{\star}(\tau;\bar{n}_{\mathrm{tx}})$ as a function of $\bar{n}_{\mathrm{tx}}$ for $\kappa \in \{0.01, 0.1, 0.25, 0.5, 0.75\}$, with operating frequency $\omega_0 = 2\pi\,400$ THz. In this figure, $G_{\mathrm{o}}^{\star}(\tau;\bar{n}_{\mathrm{tx}})$ has been obtained from (23) by numerical optimization using grid search methods. It can be observed that $G_{\mathrm{o}}^{\star}(\tau;\bar{n}_{\mathrm{tx}})$ increases by increasing the system resources $\bar{n}_{\mathrm{tx}}$. For large propagation loss (small values of κ), large system resources are needed to achieve a quantum advantage. Conversely, in the presence of high-quality channels encompassing less severe propagation loss, a quantum advantage can be achieved even by employing negligible system resources.

In Figure 2b, the optimal gain in the microwave regime $H_{\mu}^{\star}(\tau;\rho)$ shown in (31) is plotted with respect to ρ, with $\omega_0 = 2\pi\,300$ MHz. In this case $\rho > 1$ gives an optimal gain strictly larger than one and upper bounded by two, while there is no quantum advantage for $\rho \leqslant 1$.

IV. Final Remarks

This paper determines the QFI for range estimation with single-mode displaced squeezed states and quantifies the quantum advantage provided by these states compared to coherent states that do not entail quantum resources. The main findings are summarized in the following.

- We provide exact expressions for the QFI about range estimation with single-mode monochromatic displaced squeezed states, thus characterizing the theoretical limits for range estimation using such quantum resources.
- In the optical regime with large propagation loss, a meaningful quantum advantage can only be achieved by using a considerable amount of system resources, i.e., states characterized by a large average number of photons.
- In the optical regime with small propagation loss, a quantum advantage is guaranteed even with limited system resources; the quantum advantage becomes unboundedly large in the ideal case of no propagation loss.
- In the microwave regime, the effects of the displacement and squeezing operations combine additively in the optimal QFI, which is only a function of the SNR and the frequency; the gain is upper bounded by two.

APPENDIX A: GAUSSIAN STATES

Gaussian states are quantum states for which the 0-order characteristic function $\chi(\alpha_\mathrm{d}) \triangleq \mathrm{Tr}\{\boldsymbol{\Xi} \boldsymbol{D}(\alpha_\mathrm{d})\}$ takes the Gaussian form [25]

$$\chi(\alpha_\mathrm{d}) = \exp\Big\{ -\alpha_\mathrm{d}^\dagger \langle \boldsymbol{A} \rangle + \alpha_\mathrm{d} \langle \boldsymbol{A} \rangle^\dagger - \big(\frac{1}{2} + \langle \Delta \boldsymbol{A}^\dagger \Delta \boldsymbol{A} \rangle |\alpha_\mathrm{d}|^2\big) + \Re\big\{\langle \Delta \boldsymbol{A}^2 \rangle (\alpha_\mathrm{d}^\dagger)^2\big\}\Big\}, \tag{32}$$

where for an operator $\boldsymbol{F}$, $\langle \boldsymbol{F} \rangle \triangleq \mathrm{Tr}\{\boldsymbol{\Xi}\boldsymbol{F}\}$. Substituting $\alpha_\mathrm{d} = (x_\mathrm{R} + \imath x_\mathrm{I})/\sqrt{2}$ and $\boldsymbol{x} = [x_\mathrm{R}\ x_\mathrm{I}]^\mathrm{T}$ in (32), the 0-order characteristic function of a Gaussian state can be written in the form [26]

$$\chi(\boldsymbol{x}) = \exp\Big\{ -\frac{\boldsymbol{x}^\mathrm{T} \boldsymbol{\Omega} \boldsymbol{V} \boldsymbol{\Omega}^\mathrm{T} \boldsymbol{x}}{2} + \imath (\boldsymbol{\Omega} \boldsymbol{d})^\mathrm{T} \boldsymbol{x} \Big\}, \tag{33}$$

with

$$\boldsymbol{\Omega} = \begin{bmatrix} 0 & 1 \\ -1 & 0 \end{bmatrix}, \qquad \boldsymbol{d} = \begin{bmatrix} \langle \boldsymbol{Q} \rangle \\ \langle \boldsymbol{P} \rangle \end{bmatrix},$$

$$\boldsymbol{V} = \begin{bmatrix} \langle \Delta \boldsymbol{Q}^2 \rangle & \frac{\langle\, [\![\Delta \boldsymbol{Q}, \Delta \boldsymbol{P}]\!]_+ \rangle}{2} \\ \frac{\langle\, [\![\Delta \boldsymbol{Q}, \Delta \boldsymbol{P}]\!]_+ \rangle}{2} & \langle \Delta \boldsymbol{P}^2 \rangle \end{bmatrix}. \tag{34}$$

APPENDIX B: QFI OF GAUSSIAN STATES

The QFI about the parameter τ for a single-mode Gaussian state is given by [27]

$$J(\tau) = \sum_{n=0}^{3} \frac{a_n^2}{4v^2 - (-1)^n} + \Big(\frac{\partial \boldsymbol{d}}{\partial \tau}\Big)^\mathrm{T} \boldsymbol{V}^{-1} \Big(\frac{\partial \boldsymbol{d}}{\partial \tau}\Big), \tag{35}$$

where $\boldsymbol{V} = \boldsymbol{S} \left(\begin{smallmatrix} v & 0 \\ 0 & v \end{smallmatrix}\right) \boldsymbol{S}^\mathrm{T}$, and

$$a_n = 2\,\mathrm{Tr}\Big\{ \boldsymbol{S}^{-1} \frac{\partial \boldsymbol{V}}{\partial \tau} \boldsymbol{S}^{\mathrm{T}^{-1}} \boldsymbol{M}_n \Big\}, \quad n = 0, 1, 2, 3, \tag{36}$$

with $\{\boldsymbol{M}_n\}$ given in terms of Pauli matrices:

$$\boldsymbol{M}_0 = \frac{\imath \left[\begin{smallmatrix} 0 & -\imath \\ \imath & 0 \end{smallmatrix}\right]}{\sqrt{2}}, \ \boldsymbol{M}_1 = \frac{\left[\begin{smallmatrix} 1 & 0 \\ 0 & -1 \end{smallmatrix}\right]}{\sqrt{2}}, \ \boldsymbol{M}_2 = \frac{\left[\begin{smallmatrix} 1 & 0 \\ 0 & 1 \end{smallmatrix}\right]}{\sqrt{2}}, \ \boldsymbol{M}_3 = \frac{\left[\begin{smallmatrix} 0 & 1 \\ 1 & 0 \end{smallmatrix}\right]}{\sqrt{2}}.$$

APPENDIX C: QFI COMPUTATION

For space reasons, the calculation of the QFI is only sketched. The QFI calculation for Gaussian states in (35) involves the partial derivatives of the mean vector and covariance matrix of the received state given in (15). It can be checked that following relations hold

$$\boldsymbol{S}^{-1} \frac{\partial \boldsymbol{V}}{\partial \tau} \boldsymbol{S}^{\mathrm{T}^{-1}} = \kappa\, \omega_0 \begin{bmatrix} 0 & \sinh(2r_\mathrm{s}) \\ \sinh(2r_\mathrm{s}) & 0 \end{bmatrix}, \tag{37}$$

and

$$\frac{\partial \boldsymbol{d}}{\partial \tau} = \sqrt{2\kappa}\, \omega_0\, r_\mathrm{d} \begin{bmatrix} -\sin(\omega_0 \tau + \phi_\mathrm{d}) \\ \cos(\omega_0 \tau + \phi_\mathrm{d}) \end{bmatrix}. \tag{38}$$

From (36), by algebraic computation we obtain $a_i = 0$ for $i = 0, 1, 2$, and $a_3 = 2\sqrt{2}\, \kappa\, \omega_0 \sinh(2r_\mathrm{s})$. Using value of a_3 along with (37) and (38) in (35) gives the QFI in (17).

REFERENCES

[1] C. L. Degen, F. Reinhard, and P. Cappellaro, "Quantum sensing," *Rev. Mod. Phys.*, vol. 89, no. 3, p. 035002, Jul 2017.

[2] M. M. Wilde, M. Tomamichel, S. Lloyd, and M. Berta, "Gaussian hypothesis testing and quantum illumination," *Phys. Rev. Lett.*, vol. 119, p. 120501, Sep 2017.

[3] S. P. Christian Weedbrook and, R. García-Patrón, N. J. Cerf, T. C. Ralph, J. H. Shapiro, and S. Lloyd, "Gaussian quantum information," *Rev. Mod. Phys.*, vol. 84, no. 2, pp. 621–669, May 2012.

[4] Z. Wang, T. C. Ralph, R. Aguinaldo, and R. Malaney, "Exploiting spatial diversity in earth-to-satellite quantum-classical communications," 2024.

[5] A. Winter, "The capacity of the quantum multiple-access channel," *IEEE Trans. Inf. Theory*, vol. 47, no. 7, pp. 3059–3065, 2001.

[6] V. Giovannetti, S. Lloyd, and L. Maccone, "Quantum-enhanced measurements: Beating the standard quantum limit," *Science*, vol. 306, no. 5700, pp. 1330–1336, 2004.

[7] E. Polino, M. Valeri, N. Spagnolo, and F. Sciarrino, "Photonic quantum metrology," *AVS Quantum Science*, vol. 2, no. 2, p. 024703, 06 2020.

[8] C. Gerry and P. Knight, *Introductory Quantum Optics*. Cambridge University Press, 2004.

[9] R. Loudon, *The Quantum Theory of Light*. Oxford University Press, 09 2000.

[10] E. Villaseñor, M. He, Z. Wang, R. Malaney, and M. Z. Win, "Enhanced uplink quantum communication with satellites via downlink channels," *IEEE Trans. Quantum Eng.*, vol. 2, pp. 1–18, Jun. 2021.

[11] A. Giani, M. Z. Win, and A. Conti, "Quantum sensing and communication via non-Gaussian states," *IEEE J. Sel. Areas Inf. Theory*, vol. 6, 2025.

[12] Q. Zhuang and J. H. Shapiro, "Ultimate accuracy limit of quantum pulse-compression ranging," *Phys. Rev. Lett.*, vol. 128, no. 1, p. 010501, Jan 2022.

[13] M. Reichert, R. D. Candia, M. Z. Win, and M. Sanz, "Quantum-enhanced Doppler lidar," *npj Quantum Inf.*, vol. 8, no. 1, pp. 1–9, Dec. 2022, Art no. 147.

[14] M. Reichert, Q. Zhuang, and M. Sanz, "Heisenberg-limited quantum lidar for joint range and velocity estimation," *Phys. Rev. Lett.*, vol. 133, p. 130801, Sep 2024.

[15] S. Lloyd, "Enhanced sensitivity of photodetection via quantum illumination," *Science*, vol. 321, no. 5895, pp. 1463–1465, Jan. 2008.

[16] S. Pirandola and S. Lloyd, "Computable bounds for the discrimination of Gaussian states," *Phys. Rev. A*, vol. 78, no. 1, p. 012331, Jul 2008.

[17] S.-H. Tan, B. I. Erkmen, V. Giovannetti, S. Guha, S. Lloyd, L. Maccone, S. Pirandola, and J. H. Shapiro, "Quantum illumination with Gaussian states," *Phys. Rev. Lett.*, vol. 101, p. 253601, Dec 2008.

[18] G. Sorelli, N. Treps, F. Grosshans, and F. Boust, "Detecting a target with quantum entanglement," *IEEE Aerosp. Electron. Syst. Mag.*, vol. 37, no. 5, pp. 68–90, 2022.

[19] C. Oh, C. Lee, C. Rockstuhl, H. Jeong, J. Kim, H. Nha, and S.-Y. Lee, "Optimal Gaussian measurements for phase estimation in single-mode Gaussian metrology," *npj Quantum Information*, vol. 5, no. 1, pp. 1–9, Jan. 2019.

[20] Z. Huang, C. Lupo, and P. Kok, "Quantum-limited estimation of range and velocity," *Phys. Rev. X*, vol. 2, no. 3, p. 030303, Jul 2021.

[21] M. Z. Win, Y. Shen, and W. Dai, "A theoretical foundation of network localization and navigation," *Proc. IEEE*, vol. 106, no. 7, pp. 1136–1165, Jul. 2018.

[22] S. Bartoletti, W. Dai, A. Conti, and M. Z. Win, "A mathematical model for wideband ranging," *IEEE J. Sel. Topics Signal Process.*, vol. 9, no. 2, pp. 216–228, Mar. 2015.

[23] D. Dardari, A. Conti, U. J. Ferner, A. Giorgetti, and M. Z. Win, "Ranging with ultrawide bandwidth signals in multipath environments," *Proc. IEEE*, vol. 97, no. 2, pp. 404–426, Feb. 2009.

[24] R. Jonsson and R. D. Candia, "Gaussian quantum estimation of the loss parameter in a thermal environment," *J. of Phys. A: Math. and Theor.*, vol. 55, no. 38, p. 385301, Aug. 2022.

[25] S. Guerrini, M. Z. Win, and A. Conti, "Photon-varied quantum states: Unified characterization," *Phys. Rev. A*, vol. 108, p. 22425, Aug. 2023.

[26] A. Serafini, *Quantum Continuous Variables: A Primer of Theoretical Methods*. Boca Raton: CRC Press, Oct. 2017.

[27] R. Nichols, P. Liuzzo-Scorpo, P. A. Knott, and G. Adesso, "Multiparameter Gaussian quantum metrology," *Phys. Rev. A*, vol. 98, p. 012114, Jul 2018.